New a Novel Dinuclear Ruthenium(III) Complex With of 6,7-Dichloroquinoxaline-2,3-dione (DCQX) ligand: Syntheses, Spectral Characterizations, Magnetic Properties, Antimicrobial Inhibitory Activity Studies of $[Ru(DCQX)(CO)_2(EtO)]_2$ Complex.

Khalifa A. Alfallous[1]
Aboajila M. Alfallous[2]

Abstract

In the present study a complex of the general formula $[Ru(DCQX)(CO)_2(EtO)]_2$complex, (where DCQX and EtO are 6,7-dichlorolquinoxaline- 2,3-dione and ethoxo), was synthesized in one step starting with the reaction of $Ru_3(CO)_{12}$ with DCQX ligand. Initial characterization based on the elemental and mass analysis has suggested one structure (Fig. 3). The IR studies were useful in assigning the coordination modes of the ligands especially in the carbonyl region of the spectrum (Fig.2). The high-intensity bands in the UV region of the spectrum may be assigned to the $QX(O\text{-}p_\pi)\rightarrow Ru(e_g)$ and $EtO(O\text{-}p_\pi)\rightarrow Ru(e_g)$ LMCT transitions and/or $Ru(t_{2g})\rightarrow(CO_\pi)$ MLCT transition(Fig. 6). The thermogravimetric analysis gave more insight into the composition and the thermal stability of the complex(Table 2).Although, both DCQX ligand and the molybdenum complex showed antimicrobial activities, the complex inhibition to the studied microorganisms was higher.

Keywords: Quinoxaline, ruthenium complex, Metal carbonyl and Biological activity.

1. Introduction

Cisplaten is successfully used in chemotherapy, but is effective only against a narrow range of tumors [1]. The development of analogues has resulted in a few clinically useful complexes, most of which, however, are cross-resistant to Cisplaten [2]. Next to platinum, ruthenium is also used for the construction of anticancer agents [3].Many ruthenium complexes have been evaluated for the treatment of cancer, in part because ruthenium(II) and ruthenium(III) complexes exhibit relatively low ligand exchange rates, which

[1] Chemistry Department, Faculty of Science, Alasmarya Islamic University , Zliten-Libya
[2] General Department, Faculty of Denistry and Oral Surgery , Alasmarya Islamic University , Zliten-Libya

are comparable to those of platinum(II) complexes [3]. Slow ligand exchange may ensure that the drug reaches its biological target without being modified. Moreover, the various oxidation states (II, III and IV) of ruthenium are all accessible under physiological conditions [4]. In these oxidation states the ruthenium center is predominantly hexa coordinated with octahedral geometry in contrast to the square-planar geometry of platinum(II). The octahedral geometry of ruthenium compounds imposes different satiric effects upon interaction with biomolecules, which in turn may cause a different anticancer profile from Cisplaten.Recent researches working on the developments of poly nuclear ruthenium, osmium complexes are focusing on their anticancer activity. The compounds presented are often supposed to exert their anticancer activity by different modes ofaction as compared to established drugs, including newly proposed mechanisms such as enzyme inhibition, cross linking of biomacromolecules or through photo-activation, though many of the examples are also capable of binding to DNA nucleonbases [5]. Organometallic ruthenium complexes with arene ligands represent a relatively new group of ruthenium compounds with antitumor activity displayed in vitroand invivo [6]. The most hydrophobic arene ligand, showed the highest tumor-inhibiting activity. It has been suggested that thepresence of the hydrophobic planar arene ligand facilitates recognition and transport of thesecomplexes through cell membranes.

2. Experimental

trirutheniumdodecacarbonyl $Ru_3(CO)_{12}$, oxalic acid ($C_2H_2O_4.2H_2O$) and 4,5-dichloro-1,2-phenylenediamine ($C_6H_6N_2Cl_2$) were used as purchased from Sigma–Aldrich Chemical Co. Inc. 6,7-dimethylquinoxaline-2,3-dione (DCQX) ligand was synthesized following the reported procedure [7]. All Solvents used were dried according to standard procedures. Elemental analyses were performed using a Perkin–Elmer 2400 CHN elemental analyzer. Mass Spectra were obtained on a JEOL JMS-AX500 mass spectrometer.Magnetic Susceptibility measurements for the synthesized complex have been recorded on solid sample at 298 K. Thermogravimetric analysis (TGA) was carried out on a solid sample, under nitrogen atmosphere with a heating rate of 10˚C/min., using Shimadzu DT-50 thermal analyzer. The electronic absorption spectra were recorded by using Unicam UV2–300 UV–Vis spectrometer. Samples of $2.6x10^{-4}$mol dm^{-3} concentrations in DMSO were measured against the solvent in the reference cell. Antimicrobial activity of the tested samples for the ligand and the complex was determined using a modified Kirby-Bauer disc

diffusion method [8]. A 100 μL of the test bacteria or fungi were grown in 10 mL of fresh media until they reach a count of an approximately 108 cells/mL for bacteria and an approximately 105 cells/mL for fungi. A 100 μL of microbial suspension was spread onto agar plates corresponding to the broth in which they were maintained. Plates inoculated with Gram-positive bacteria (Staphylococcus aureus) and Gram-negative bacteria (Escherichia Coli) were incubated at 35–37 ˚C for 24–48 h. Whereas, filamentous fungus (Aspergillusflavus) and yeast fungus (Candida albicans) were incubated at 25 ˚C for 48 h and 30 ˚C for 24–48 h, respectively. Then the diameters of the inhibition zones were measured in millimeters. Standard discs of tetracycline (antibacterial agent) and Amphotericin (antifungal agent) served as positive control for antimicrobial activity, while filter discs impregnated with 10 μL of DMSO solvent were used as a negative control. Blank paper discs with a diameter of 8.0 mm were impregnated with 10 μL of the tested samples stock solution (0.02 g/mL) and inhibition zone diameters were measured.

2.1. Synthesis of $[Ru(DCQX)(CO)_2(EtO)]_2$ complex :

$Ru_3(CO)_{12}$ (0.10 g, 0.156 mmol) and DCQX (0.108 g, 0.470 mmol) are mixed in about 50 ml THF. The solution was reflux under atmospheric pressure for 6 hours with continuous stirring, and during this time brown solid of the product separated from solution. The solid was isolated, washed with 15 mL THF/EtOH (1:1) and dried in vacuum. A concentrated solution of the product in DMSO/EtOH (3:1) was allowed to evaporate slowly for 2 week and has resulted in reddish-brown powder. Washing the powdery solid with EtOH followed by diethyl ether and then dried overnight in vacuum, has resulted in 0.087 g (42.9 % yield) of the product. Anal. Calc. for $C_{24}H_{18}Cl_4Ru_2N_4O_{10}$ (Mr = 866.42): C, 33.27; H, 2.09; Cl, 16.37; N, 6.47. Found: C, 32.90; H, 2.21; Cl, 15.61; N, 6.19%. Effective magnetic moment at 298 K, μ_{eff} (BM): 1.046.

3. Results and Discussion

The mass spectra of the complex shown in (**Fig. 1**) exhibited parent peaks due to molecular ions $[M]^+$ and $[M+1]^+$ at (m/z) values of 865.85 and 865.8; respectively. Fragments corresponding to the molecular ions $[M\text{-}CO]^+$, $[M\text{-}2CO]^+$, $[M\text{-}3CO]^+$ and $[M\text{-}4CO]^+$ were observed for the complex at (m/z) values of 837.85, 809.75, 782.92 and 753.65; respectively. Fragments corresponding to the molecular ions $[M\text{-}QX]^+$, $[M\text{-}2QX]^+$, $[M\text{-}2QX\text{-}2CO]^+$, $[M\text{-}2QX\text{-}3CO]^+$ and $[M\text{-}2QX\text{-}4CO]^+$ were observed for the complex at (m/z) values of 643.14, 404.80, 343.90, 219.5 and 290.24; respectively.

Fragments corresponding to half the molecular weight of the complex were observed in the mass spectra at m/z values of 434.14. Other fragment that can be attributed to $[Ru(OEt)_2Ru]$ unit was observed for the complex at 246.34. These results may suggest dinuclear ruthenium complex with the two Ru centers connected together by di-μ-ethoxo groups and each Ru metal bonded to a DCQX and di carbonyl groups.

The infrared studies of the synthesized complex were useful in assigning the coordination mode of the DCQX ligand to the ruthenium metal centers. The main characteristic feature of the IR spectra of the dinuclear complex (**Fig. 2)** was the disappearance of the bands corresponding to the C=O stretches and the presence of a new band corresponding to coordinate C–O group. In addition, a new band due to non-conjugated C=C was observed at 1618 cm^{-1}. The observed values for C–O stretching vibrations in good agreement with those reported for *o*-catecholates ligands coordinated to transition metal ions [9-11]. Another important feature of the IR spectra of the complex was three bands characteristic of μ-ethoxo ligands observed at 1112, 1076 and 872 cm^{-1} for complex [12]. Bands that can be attributed to the stretching vibrations of the Ru-O(DCQX) and Ru-O(EtO) were observed at 576 and 474 cm^{-1}, respectively. Moreover, the infrared spectrum in the carbonyl region revealed three bands at 2040, 1990 and 1953 cm^{-1}(**Table 1**). Their values in combination with the mass spectroscopic results suggest four terminal CO groups are arranged around the two Ru metal centers in such a way that either two of them, on one Ru metal or on two Ru metals, are in trans-position to one another. The results obtained from the mass and infrared studies suggest a structure of the ruthenium complex with four carbonyl ligands on each Ru(III) metal center as shown in **Figure 3**.

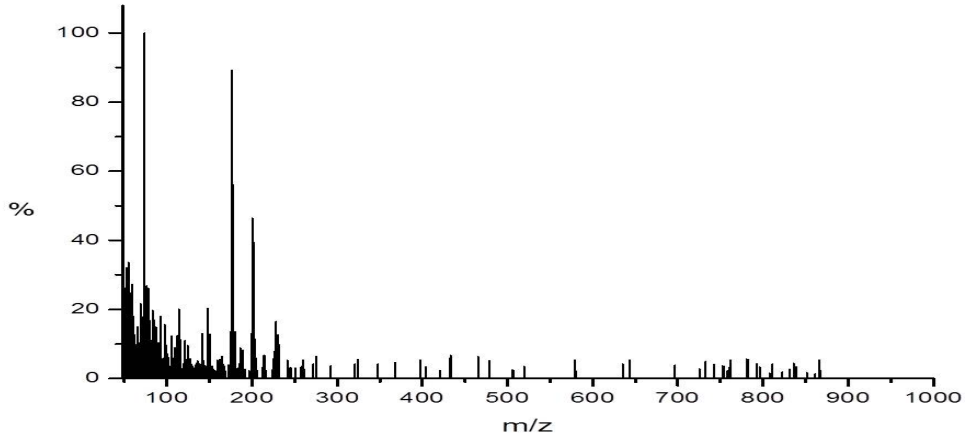

Fig. 1. The mass spectrum of [Ru(DCQX) $(CO)_2(EtO)]_2$ complex

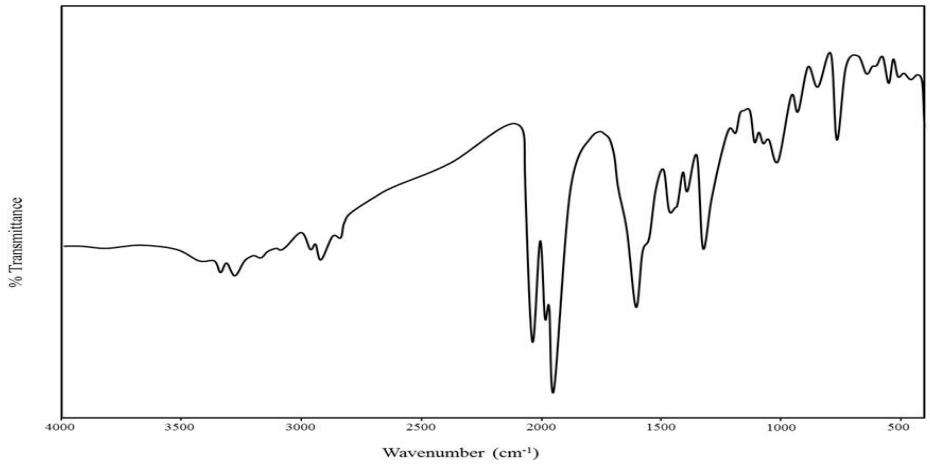

Fig. 2. The IR spectrum of [Ru(DCQX)$(CO)_2(EtO)]_2$ complex.

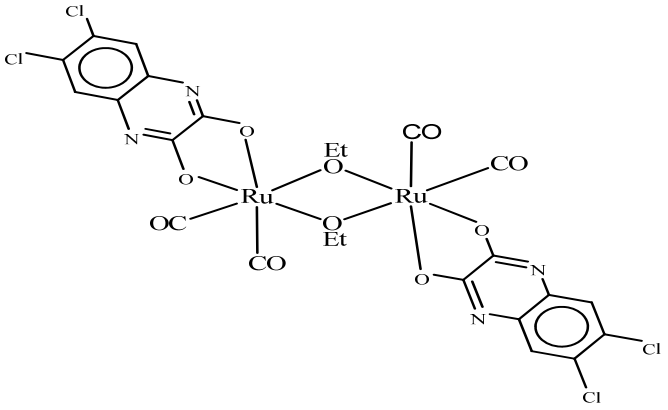

Fig. 3. Suggested structure for the $[Ru(DCQX)(CO)_2(EtO)]_2$ complex.

Table 1. : Characteristic calculated and observed vibrational frequencies (cm^{-1}) for the $[Ru(DCQX)(CO)_2(OEt)]_2$ complex

Vibrational Frequencies (cm^{-1})[a] $[Ru(DCQX)(CO)2(OEt)]_2$		Assignment
Calcd	**Obsd**	
3344.9	3345(w,b)	ν_{asymm}N–H
3280.4	3282(w,b)	ν_{symm}N–H
3132.8	3133(w,b)	νC–H aromatic rings (DCQX)
3092.3	3089(w,b)	νC–H aromatic rings (DCQX)
2958.7	2966(sh)	νC–H (EtO)
2920.3	2924(m)	νC–H (EtO)
2838.5	2843(sh)	νC–H (EtO)
2053.4	2040(vs)	νCO (asymm axial, asymm equatorial)
1998.0	1990(sh)	νCO (symm axial, asymm equatorial)
1950.7	1953(vs)	νCO (asymm axial, symm equatorial)
1622.0	1618(s)	νC=C heterocyclic ring
1483.1	1475(m)	νC=C aromatic + ringdeformation (DCQX)
1469.4	1490.9(s)	νC=C aromatic + ringdeformation (DCQX)
1406.3	1402(m)	γC–H (EtO)
1344.6	1335(s)	$\nu C–O_{asymm}$ (DCQX)
1193.4	1213(w)	δC–H (DCQX)
1250.1	1246.3(s)	νC–O (QX)
1114.8	1112(w)	ν_{asymm}C–O (EtO)
1086.7	1076(w)	ν_{symm}C–O (EtO)
871.2	872(m)	δC–O (EtO)
785.9	789(s)	$\delta_{asymm}RuO_2Ru$ ring
665.6	665(w)	ν_{asymm}O (DCQX)–Ru–O(EtO)
571.8	576(m)	νRu–O (EtO)
477.8	474(w)	νRu–O (DCQX)

[a]w, weak; m, medium; s, strong; vs, very strong; b, broad

Magnetic Susceptibility measurements for the synthesized complex have been recorded on solid sample at 298 K and have revealed effective magnetic moments of 1.046 BM. The spin-only value expected for two non-interacting low-spin Ru(III) metal (S = ½) is 1.37. Consequently, the significantly lower

value of the observed magnetic moment indicates a strong antiferromagnetic coupling between two low-spin Ru(III) metal ions . However, the lower value of the magnetic moment for low-spin d^5 (S = 1/2) systems, is not unusual for dinuclear Ru(III) complexes [13].

The X-band EPR spectrum recorded for a powder sample of the complex is depicted in **figure 4**. The exchange interaction between the two low-spin Ru(III) metals is expected to be similar to the exchange coupling between two Cu(II)-containing molecules with axial pattern spectrum [14]. The triplet state S = 1 was simulated using easy-spin software. The axial pattern esr spectrum of complex (**Fig. 4**) was simulated with the parameters J = 630 cm^{-1}, $g_{\square}$ = 2.01, $g_{\perp}$= 2.048 for Ru(1) and $g_{\square}$ = 1.973, $g_{\perp}$= 2.181 for Ru(1′) with D = 0.167 cm^{-1} and E =0.012 cm^{-1}. The higher value of the calculated coupling constant (J = 630 cm^{-1}) is in good agreement with the Ru-O-Ru angles and Ru…Ru separation obtained by the parameterized PM3 semiempirical calculations [15]. It was reported, two isomers for the low-spin dinuclear Ru(III) complex, $[C_5(CH_3)_5Ru(\mu\text{-}Cl)Cl]_2$, where the isomer with Ru…Ru separation of 2.93 Å and Ru(III)-Cl-Ru angle of 76° displayed a strong antiferromagnetic coupling J = 670 cm^{-1}[142]. On other hand, the isomer with Ru…Ru separation and Ru-Cl-Ru angle values of 3.75 cm^{-1} and 100° has shown weak coupling between the two Ru(III) metals with J = 24 cm^{-1}.

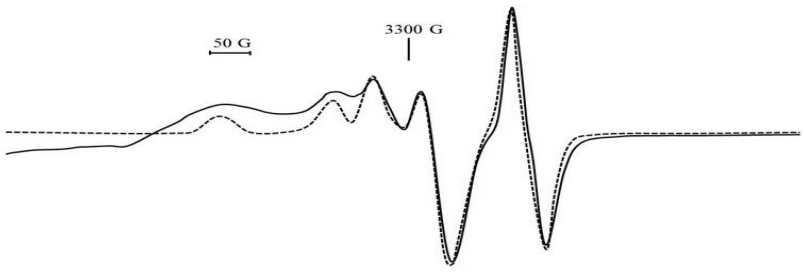

Fig. 4 : X-band EPR spectra of $[Ru(DCQX)(CO)_2(EtO)]_2$complex: Solid curve: experimental spectrum measured onpowder sample at 298 K. Dotted curve: simulated spectrum with the parameters J = 630 cm^{-1}, $g_{\square}$ = 2.01, $g_{\perp}$= 2.048 for Ru(1) and $g_{\square}$ = 1.973, $g_{\perp}$= 2.181 for Ru(1′) with D = 0.167 cm^{-1} and E =0.012 cm^{-1}

The data for thermal analysis (TGA), carried out on a solid sample of the $[Ru(DCQX)(CO)_2(EtO)]_2$ complex in the temperature range 20–1000

°C at heating rate of 10 °C/min. under nitrogen atmosphere, shown in **Figure 5**, revealed four decomposition steps. The first step showed slow decomposition up to 185 °C with a net weight loss of 10.81% which is most probably due to loss of the C_2H_5 of the two ethoxo groups and one chlorine atom from the DCQX ligand (**Table 2**). This is followed by gradual decomposition of mainly $Cl_2C_6H_2N_2H_2C_2$ of the other DCQX ligand in the temperature range 191-299 °C. The decompositions of the 4CO molecules were observed in the temperature range 299-382°C. The last step covers the temperature range of 382-476 °C with the elimination of the remaining of the (DCQX) ligand. The remaining residue was found 30.77% which is best ascribed to Ru_2O_3.

Table 2. Thermal analysis data for $[Ru(DCQX)(CO)_2(EtO)]_2$ complex

Decomposition Steps, °C	% weight loss	Molecular weight (found)	Molecular weight (Calced.)	Assigned species
52-191	10.81	93.68	93.57	2 Et + 1 Cl
191-299	23.19	200.94	201.04	Cl2-C6H2-N2H2-C2 (of DCQX)
299-382	17.12	148.38	148.49	4 CO + 1Cl + H
476-995	18.08	156.72	157.10	C6H-N2-C2-O2 (of DCQX)

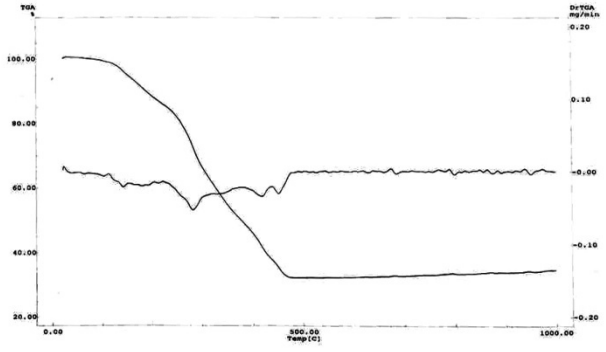

Fig. 5. The TGA thermogram of $[Ru(DCQX)(CO)_2(EtO)]_2$ complex.

The electronic absorption spectra of the dinuclear Ru(III) complex was recorded as a solution in DMSO at room temperature in the region 200-1050 nm and the spectrum is show in **Figure 6**. In similarity to the electronic spectra of the dinuclear Cr(III) complexes, $[Cr(bpy)(QX)EtO]_2$

[16]. The spectrum of the dinuclear Ru(III) complex showed high intensity-broad absorptions in the UV region, two-weaker broad bands in the visible regionand very low-intensity multiple maxima in the 600-725 nm region. However, the shifts in the position of the absorption band maxima may reflect the difference in energies of the orbitals originating these transitions in the complex in addition to occupancy of the t_{2g} orbitals which might affect the MLCT or LMCT transitions. The very weak maxima observed in spectra between 600-725 nm are characteristic of spin-forbidden d-d transitions of diametric complexes [17]. The high-intensity bands in the UV region of the spectrum may be assigned to the QX(O-p_π)→Ru(e_g) and EtO(O-p_π)→Ru(e_g) LMCT transitions and/or Ru(t_{2g})→(CO_π) MLCT transition. The ground state of the low-spin ruthenium(III) is $^2T_{2g}$ and the excited doublet levels in the order of increasing energy would be $^2A_{2g}$ and $^2T_{1g}$[18]. Therefore, the two weaker bands in the visible region can be assigned to $^2T_{2g}\rightarrow{}^2A_{2g}$ and $^2T_{2g}\rightarrow{}^2T_{1g}$ transitions with the possible charge transfer transitions. Consistence with these assignments the dinuclear Ru(III) complex, $[Ru_2LCl_4]Cl_2$(L = 3,6-dimethyl-4,5-diazaocta-3,5-diene-2,7-dione) showed three absorption bands at 438, 568 and 760 nm corresponding to the spin-allowed $^2T_{2g}\rightarrow{}^2A_{2g}$ and $^2T_{2g}\rightarrow{}^2T_{1g}$ transitions and the spin-forbidden $^2T_{2g}\rightarrow{}^4T_{2g}$, and $^4T_{1g}$ [19].

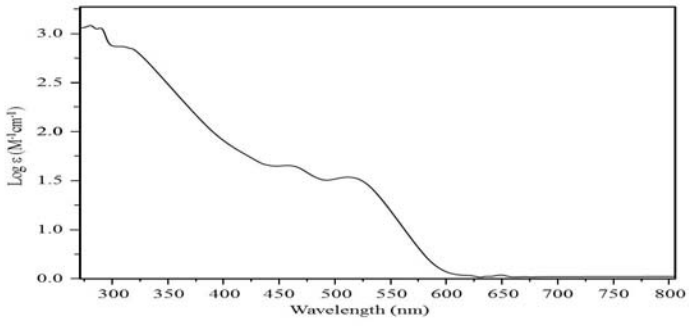

Fig. 6. The UV-vis spectrum of $[Ru(DCQX)(CO)_2(EtO)]_2$ complex in DMSO.

4. Antimicrobial Activity of ruthenium complex:

The antimicrobial activities of the DCQX and DMQX Ligands and ruthenium complexes were tested by the disc diffusion method against two types of pathogenic bacteria, namely, S. aureus and E. Coli by using DMSO as a solvent and tetracycline as a standard antibacterial agent. While the antifungal activity for the free ligand and the complex were tested against A. flavus and C. albicans fungi using Amphotericin as a standard antifungal agent. The maeasured inhibition zone diameters for the ruthenium complexes and their free ligands are presented in **Table 3**.

The results indicated that both DCQX and DMQX ligands, $[Ru(DCQX)(CO)_2(EtO)]_2$ and $Ru_3(DMQX)_2(CO)_4(C_6H_6)_2$ complexes show biological activities against both bacteria and fungi. Surprisingly, the two complexes showed similar antibacterial activities whereas, only the triruthenium complex showed antifugual activity against candida albicans. Nevertheless, we believe that these ruthenium complexes can show anticancer activities which is worth to try [20].

In conclusion, the data of the biological activity studies of both complex indicated higher antimicrobial inhibitory activities (bacterial and fungual) for $[Ru(DCQX)(CO)_2(EtO)]_2$complex showed only higher antifungal inhibitory activities compared with that of the free DCQX ligand.

Table3. Antimicrobial Activities of ruthenium complex.

Sample	Inhibition zone diameter (mm/mg sample)			
	Escherichia Coli (gram-negative)	**Staphylococcus aureus (gram-positive)**	**Aspergillus Flavus**	**Candida Albicans**
DMSO[a]	0.0	0.0	0.0	0.0
Tetracycline [b]	31	33	-	-
Amphotericin B[c]	-	-	17	21
DCQX	15	16	12	12
$[Ru(DCQX)(CO)_2(EtO)]_2$	14	15	0.0	0.0

[a] DMSO solvent was used as negative control.
[b] Standard antibacterial agent.
[c] Standard antifungal agent.

References

[1] B. Lippert, Cisplatin. Chemistry and Biochemistry of a Leading Anticancer Drug, VerlagHelvetica Chimica. Acta, Zurich, Wiley-VCH, Weinheim, 1999.

[2] M. A. Jakupec,M. Galanski, B. K. Keppler, Rev. Physiol. Biochem. Pharmacol.146 (2003) 1-53.

[3] M. J. Clarke, Coord. Chem. Rev. 236 (2003) 209-233.

[4] C. S. Allardyce, P. J. Dyson, Plat. Met. Rev.45 (2001) 62-69.

[5] C. G. Hartinger, A. D. Phillips, A. A. Nazarov, Curr. Top. Med. Chem. 21 (2011) 2688-2702.
[6] A. E. Aird, J. Cummings, A. A. Ritchie, M. Muir, R. E. Morris, H. Chen, P. J. Sadler, H. Jodrell, Br. J. Cancer 86(2002) 1652-1657.
[7] H. Thakuria, G. Das, J. Chem. Sci. 118 (2006) 425.
[8] F. Dianzhong, M.Wang, B.Wang, Polyhedron 11 (1992) 1109.
[9] P. A. Wicklund, D. G. Brown, Inorg. Chem 15 (1976) 396-401.
[10] D. G. Brown, W. L. Johnson, Z. Naturforsch. 34B (1979)712-716.
[11] A. S. Attia, Polyhedron 26 (2007) 2550-2558.
[12] C. S. Wu, G. R. Rossman, H. B. Gray, G. S. Hammond, H. J. Schugar, Inorg. Chem. 11 (1972) 990-994.
[13] M. Mikuriya, D. Yoshioka, M. Handab, Coord. Chem. Rev. 250 (2006) 2194–221.
[14] W. Wang, X. Liu, D. Liao, Z. Jiang, S. Yan, G. Wang, Inorg. Chem. Comm. 5 (2002) 1007–1011.
[15] G. Ertepinarl, Y. Gok, O. Geban, S. Ozden, Eur. J. Med. Chem. 30 (1995) 171-175.
[16] Attia S. Attia , Ayman A. Abdel Aziz, Khalifa A. Alfallous, M.F.El-Shahat,Polyhedron 51 (2013) 234-254.
[17] K.N. Raymond, S. S. Isied, L. D. Brown, F. R. Fronczek, J. H. Nibert, J. Am. Chem. Soc., 98 (1976) 1767-1774.
[18] A.Khalafi-Nezhad, M. N. Soltani Rad, H. Mohalbatkar, Z. Asrsri, B. Hemmateenejad, Bioorg. Med. Chem. 13 (2005) 1931-1938.
[19] A.K. Ghose, A. Pritchet, G. M. Crippen, J. Comput. Chem. 9 (1988) 80-90.
[20] F. A. Peacock, P. J. Sadler Medicinal organometallic chemistry: designing metal arene complexes as anticancer agents. Chem.Asian. J. 3 (2008) 1890–1899.